NORSAR

Scientific Report No. 2-82/83

SEMIANNUAL TECHNICAL SUMMARY
1 October 1982 — 31 March 1983

Linda B. Tronrud (ed.)

Kjeller, June 1983

VI.2 The present seismic evidence for a boundary layer at the base of
      the mantle

The velocity structure at the base of the mantle has been the subject of
a long-standing controversy. Velocity models proposed in the past encompass
a range from positive to negative gradients; the three models shown in
Fig. VI.2.1 are representative of different alternatives. This figure
also shows two different interpretations of combined P and S velocity
profiles, as a density effect or as a temperature effect. Note that models
with velocities which are anomalous in the sense that the gradients with
depth reverse and become negative, have recently been associated with a
thermal boundary layer. In 1974, Cleary reviewed the available seismic
evidence and concluded that a velocity reversal was likely. However, the
data were interpreted mainly in a ray geometrical context and since dif-
fraction effects can be significant, the evidence has been subject to
criticism. Doornbos and Mondt (1979) applied diffraction theory to an
extensive set of long-period P and SH data and still inferred a velocity
reversal, although the thickness of the low-velocity zone was found to
be much smaller than the 200 km conventionally assign to the D" layer.
More recently, several authors find no evidence for a low-velocity zone
(see, e.g., Ruff and Helmberger, 1982). In a recent contribution we have
made use of new data from the SRO network and from the NORSAR array,
in an attempt to reconcile the available evidence.

A typical example of long-period diffracted waves observed at the SRO
network, is shown in Fig. VI.2.2. It is clear that the amplitude decay
of SV in the core shadow zone is too strong to yield useful data, in
agreement with a theoretical prediction for a range of possible models.
Thus, only P and SH have been used here. Some striking examples of short-
period diffracted P at the NORSAR array are given in Fig. VI.2.3. PKP
from the same events are given for comparison, and the data to be used
are based on an amplitude ratio of P and PKP at the periods 1 and 2
seconds. Altogether we have obtained long-period diffraction data from
16 events, long-period P from 25 events, and short-period P from 10
events.

In Figs. VI.2.4 and VI.2.5 the data are compared to calculated decay spectra and dT/dΔ, using the models of Fig. VI.2.1. In the calculations, the extended WKBJ method (Langer's approximation) was applied to a piecewise smooth layered model. In this way the effect of both a velocity gradient and changes in the gradient are evaluated (Doornbos, 1981). The dT/dΔ curves of Fig. VI.2.4 reflect the fact that diffracted waves are usually dispersed. In analogy to phase and group velocity, we have introduced the phase and group slowness, $p(\omega)$ and $g(\omega)$, respectively. Their difference is

$$g(\omega) - p(\omega) = \omega\ dp/d\omega$$

and since this dispersion depends on the velocity gradient and its changes, it can be used as an additional diagnostic.

The observed low decay of long-period diffracted SH, the dT/dΔ values, and the apparent absence of dispersion, are all compatible with a relatively thin (< 100 km) low-velocity zone for S at the base of the mantle. The long-period SRO data lack the resolving power to settle the question for P. The results for short-period P as summarized in Fig. VI.2.5 strongly suggest that a comparable low-velocity zone for P exists, at least in the region sampled by the NORSAR data (beneath Central Asia). It is not inconsistent with a global average of short-period dT/dΔ and amplitude data near the core shadow boundary (also summarized in Fig. VI.2.5), but it should be mentioned that at least one recent study of short-period amplitudes gave results conflicting with the global average (Ruff and Helmberger, 1982). If this is to be 'explained' by lateral variations, then it should be added that the presence of lateral variations itself is not in conflict with boundary layer models. On balance, current thermal models appear to be consistent with (but not required by) the present seismic evidence.

D.J. Doornbos

References

Cleary, J.R. (1974): The D" region, Phys. Earth Planet. Int. 9, 13-27.

Doornbos, D.J. (1981): The effect of a second-order velocity discontinuity on elastic waves near their turning point, Geophys. J.R. Astr. Soc. 64, 499-511.

Doornbos, D.J. and J.C. Mondt (1979): P and S waves diffracted around the core and the velocity structure at the base of the mantle, Geophys. J.R. Astr. Soc. 57, 381-395.

Ruff, L.J. and D.V. Helmberger (1982): The structure of the lowermost mantle determined by short-period P-wave amplitudes, Geophys. J.R. Astr. Soc. 68, 95-119.
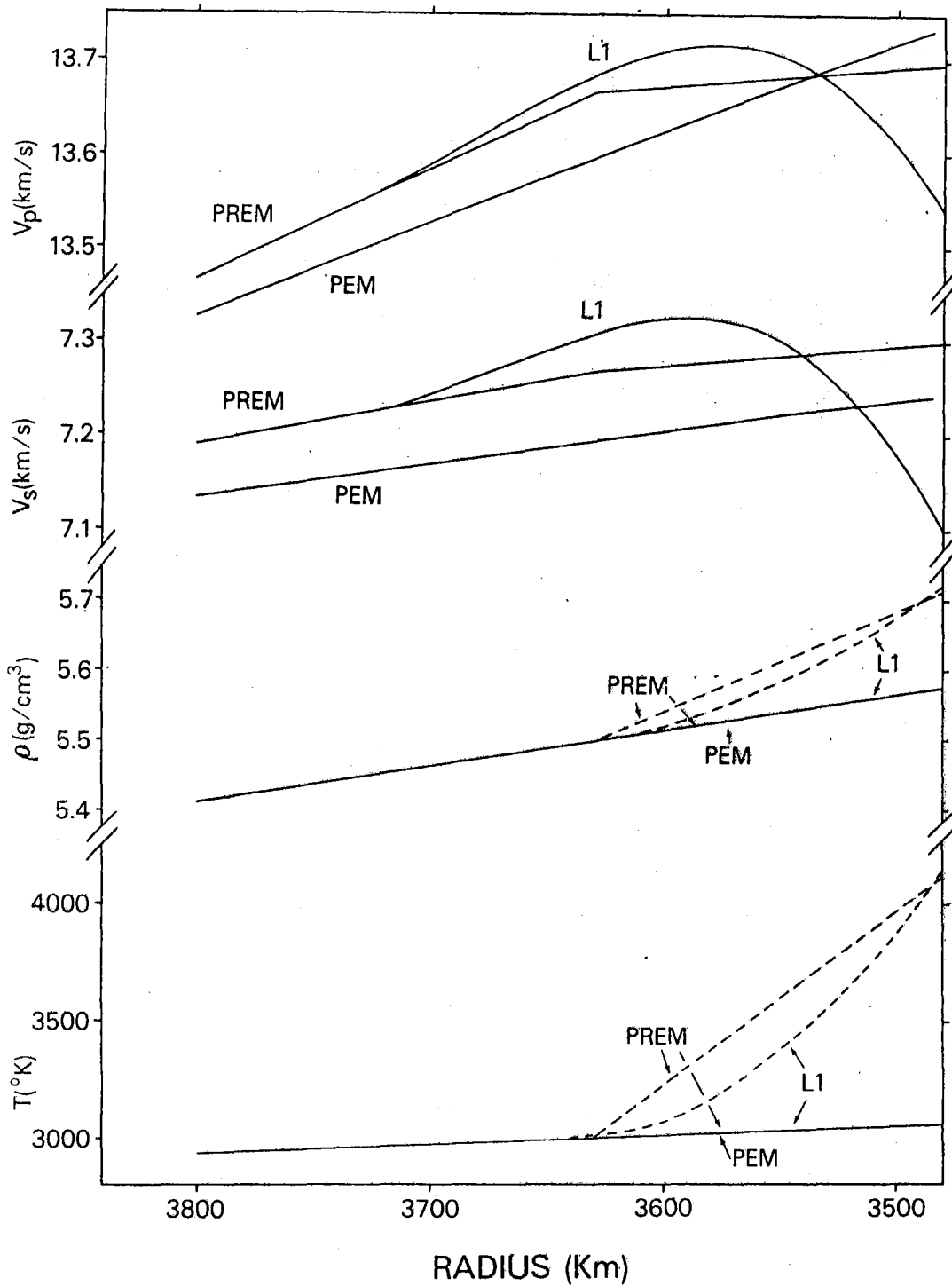
Fig. VI.2.1   Models of P and S velocity v_p, v_s, density ρ and temperature T
in the lower mantle. The superdiabatic temperature profiles
of PREM and L1 correspond to a homogeneous density (PEM
profile), and the inhomogeneous density profiles correspond
to the adiabatic temperature of PEM. Absolute temperatures
have been arbitrarily fixed.

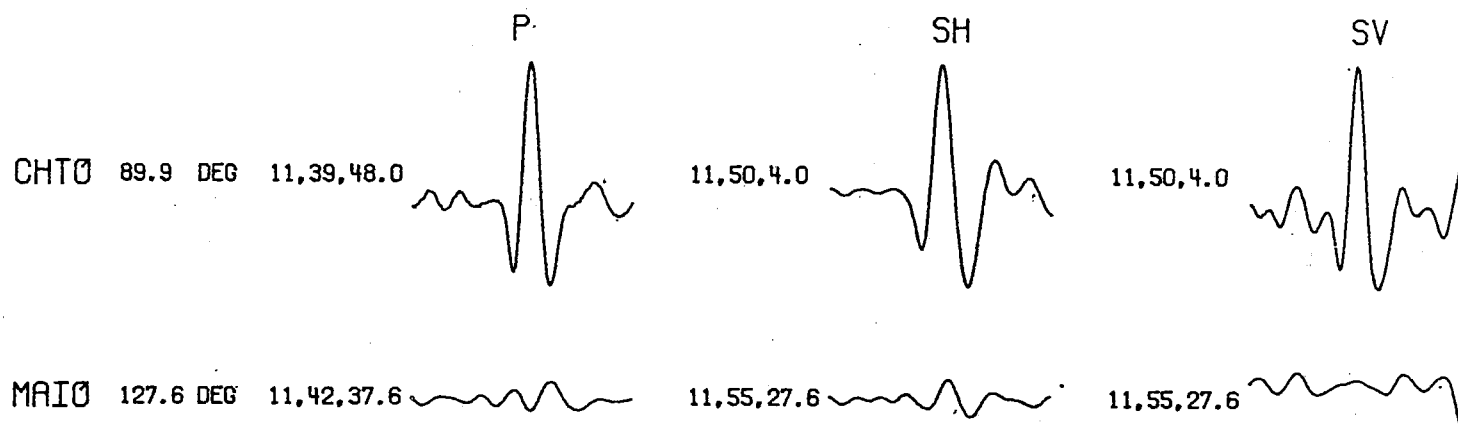ORIGIN TIME 1977 JULY 6, 11 HR, 28 MIN, 31.5 SEC, DEPTH=594KM, MB=5.8, FIJI IS.

P.   SH   SV

CHTO   89.9 DEG   11,39,48.0   11,50,4.0   11,50,4.0

MAIO   127.6 DEG   11,42,37.6   11,55,27.6   11,55,27.6

Fig. VI.2.2   Vertical, radial and transverse component SRO records of P, SV, and SH near
              a great circle path around the core. Time length is 2 minutes.

DELTA = 130.4 DEG   P
DEPTH = 200   KM

DELTA = 130.4 DEG   PKP
DEPTH = 200   KM

400 c.

DELTA = 132.1 DEG   P
DEPTH = 45   KM

DELTA = 132.1 DEG   PKP
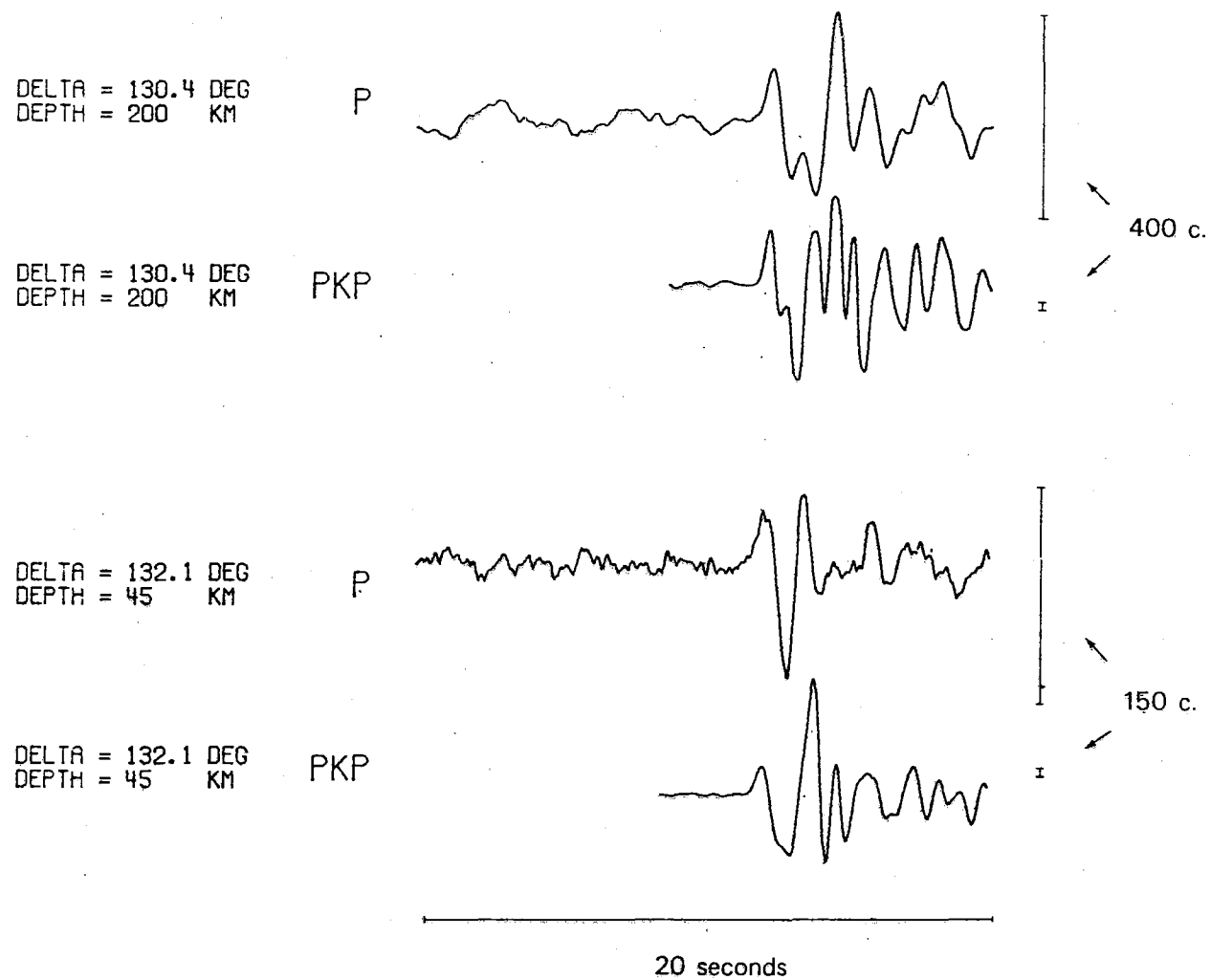DEPTH = 45   KM

150 c.

20 seconds

Fig. VI.2.3   NORSAR array beams of short-period P and PKP for two events in the Solomon Islands region (1983, Aug 1 and Nov 30). Time length is 12 seconds.
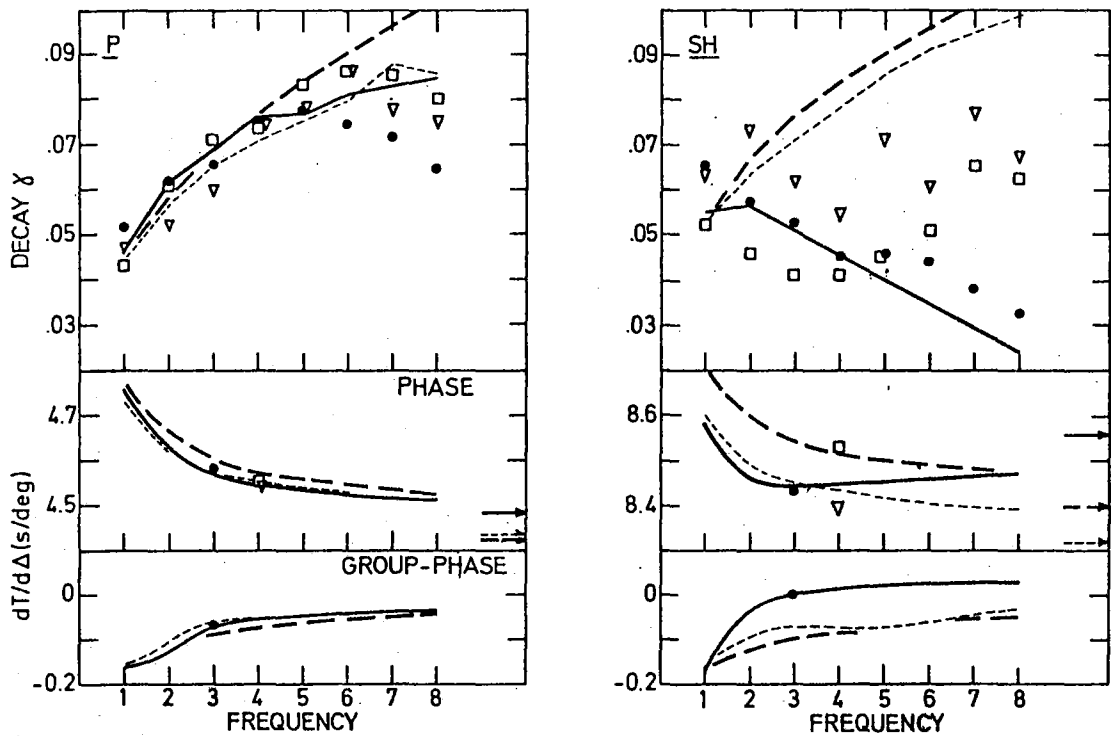
Fig. VI.2.4   Decay spectra and dT/dΔ of P and SH. The decay γ measures
logarithmic amplitude decay per degree of epicentral dis-
tance and corrected for geometrical spreading. Group-phase
slowness is a measure of dispersion. Frequency point 1,...,8
correspond to 0.015625,....,0.125 Hz in steps of 0.015625.
Theoretical curves for models ____ __ : PEM; _ _ _ _ : PREM;
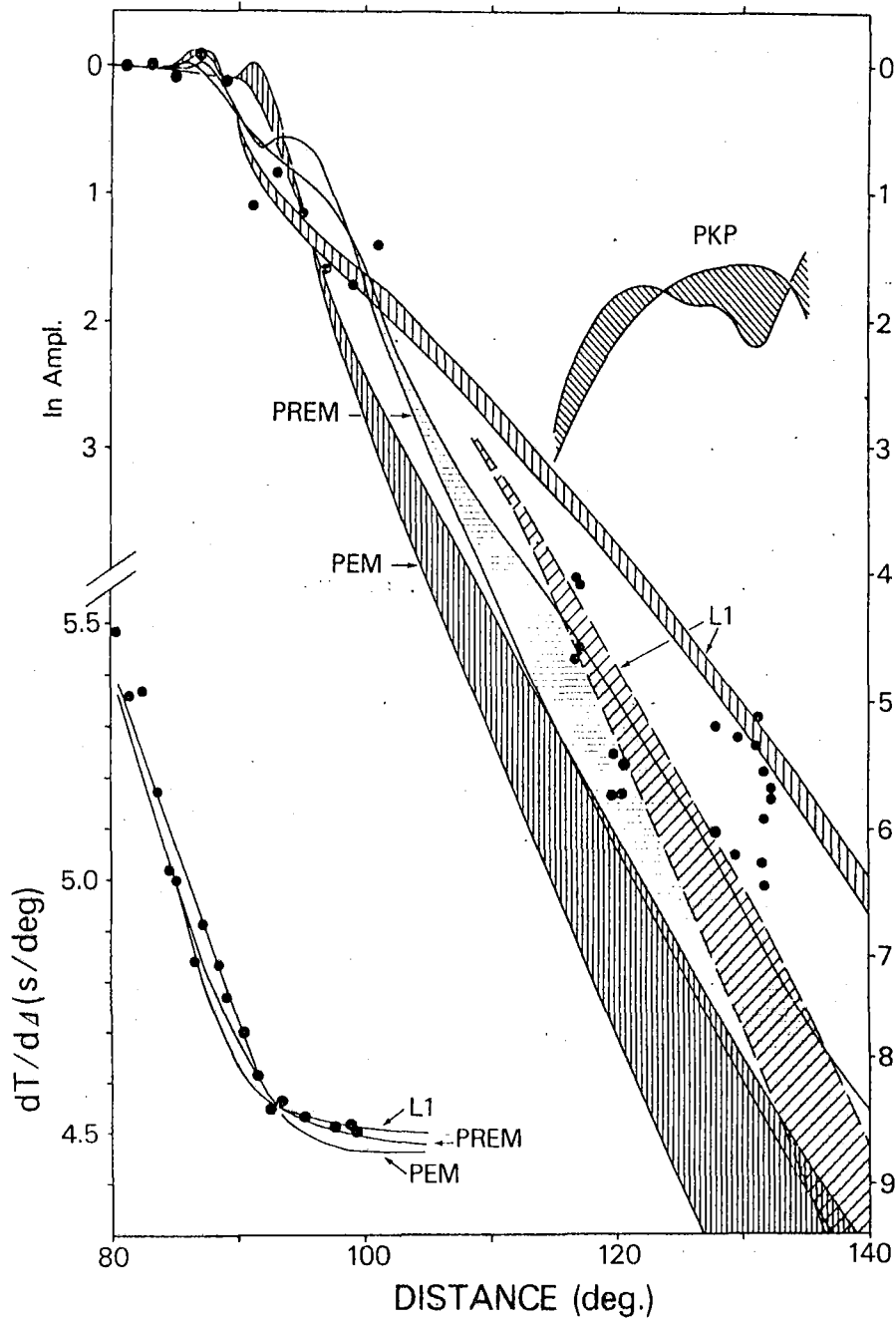_____ : L1. Averaged observational data ● : this study;
□ and ∇ : other studies.

Fig. VI.2.5 dT/dΔ and relative amplitudes of short-period P. Theoretical
curves for models PEM, PREM and Ll. Amplitude bands correspond
to period range 1-2 seconds. Additional amplitude decay due
to anelastic damping indicated for model Ll with Q_α = 400 at
base of mantle. Amplitude data between 115-135° are from NORSAR
(this study). Amplitude and dT/dΔ data between 80-105° are from
other studies.